Research Article


# Mechano-chemo signaling interactions modulate matrix production by cardiac fibroblasts

**Jesse D. Rogers [a], Jeffrey W. Holmes [b], Jeffrey J. Saucerman [c] and William J. Richardson [a,*]**

***a* - Department of Bioengineering,** *Clemson University, Clemson, SC, USA*
***b* - Departments of Biomedical Engineering,** *Medicine/Cardiovascular Disease, and Surgery/Cardiothoracic Surgery, University of Alabama at Birmingham, Birmingham, AL, USA*
***c* - Department of Biomedical Engineering and Robert M. Berne Cardiovascular Research Center,** *University of Virginia, Charlottesville, VA, USA*

***Correspondence to William J. Richardson:*** *Department of Bioengineering, Clemson University, 301 Rhodes Research Center, Clemson, SC 29634, USA. wricha4@clemson.edu*
https://doi.org/10.1016/j.mbplus.2020.100055

## Abstract

Extracellular matrix remodeling after myocardial infarction occurs in a dynamic environment in which local mechanical stresses and biochemical signaling species stimulate the accumulation of collagen-rich scar tissue. It is well-known that cardiac fibroblasts regulate post-infarction matrix turnover by secreting matrix proteins, proteases, and protease inhibitors in response to both biochemical stimuli and mechanical stretch, but how these stimuli act together to dictate cellular responses is still unclear. We developed a screen of cardiac fibroblast-secreted proteins in response to combinations of biochemical agonists and cyclic uniaxial stretch in order to elucidate the relationships between stretch, biochemical signaling, and cardiac matrix turnover. We found that stretch significantly synergized with biochemical agonists to inhibit the secretion of matrix metalloproteinases, with stretch either amplifying protease suppression by individual agonists or antagonizing agonist-driven upregulation of protease expression. Stretch also modulated fibroblast sensitivity towards biochemical agonists by either sensitizing cells towards agonists that suppress protease secretion or de-sensitizing cells towards agonists that upregulate protease secretion. These findings suggest that the mechanical environment can significantly alter fibrosis-related signaling in cardiac fibroblasts, suggesting caution when extrapolating in vitro data to predict effects of fibrosis-related cytokines in situations like myocardial infarction where mechanical stretch occurs.


## Introduction

Myocardial infarction (MI) affects a significant proportion of the US population, with approximately 8 million adults diagnosed from 2011 to 2014 [1]. Although short-term outcomes have improved with the widespread adoption of percutaneous coronary intervention and reduced response times [2], maladaptive scar tissue formation in the myocardium can lead to serious post-MI complications such as cardiac rupture, infarct expansion, or heart failure. These complications are dependent on a balance between tissue formation by the synthesis of extracellular matrix (ECM) and tissue degradation by a variety of proteases including matrix metalloproteinases (MMPs). While ECM synthesis is desirable at the infarct site for maintaining the structural integrity necessary to prevent cardiac rupture, excessive matrix accumulation can reduce systolic and diastolic function by

increasing wall stiffness and decreasing wall conductivity, resulting in progression to heart failure [3]. Thus, controlling local ECM turnover is an essential component in promoting healthy scar formation post-MI.

Cardiac fibroblasts mediate the fibrotic response to injury by assuming an activated phenotype and synthesizing both matrix proteins and proteases, thereby controlling the balance in matrix turnover to form collagenous scar tissue [4]. Fibroblasts are highly responsive to post-infarct biochemical cues consisting of pro-inflammatory cytokines, growth factors, and hormonal agents that stimulate fibroblasts to degrade or deposit ECM [5]. A growing body of research has also shown that fibroblast functionality is dependent on local mechanical cues; MI-induced loss of cardiomyocytes results in increased circumferential stretch at the infarct [6–8], which stimulates fibroblast activation through several mechano-sensing mechanisms [9]. While biochemical and mechanical signaling pathways have been studied individually in cardiac fibroblasts, few studies have examined the interplay between biochemical and mechanical signaling. Previous studies have shown that cytokine-stretch combinations can alter fibroblast activation beyond either cytokine or stretch treatment alone [10,11], but several questions remain regarding the role of stretch within the context of biochemical signaling, such as the relative contribution of stretch towards fibrosis compared to biochemical agonists and the ability of stretch to regulate biochemical signaling.

In this study, we address these questions by assessing the effects of six different biochemical agonists on cardiac fibroblast behavior in different mechanical contexts. Using a multi-well cell stretching device, we subjected adult mouse cardiac fibroblast (mCF)-seeded fibrin gels to multiple doses of each agonist under static conditions or cyclic stretch. By measuring the secretion of 13 fibrosis-regulating proteins across all mechano-chemo combinations, we examined how stretch contributes to overall fibrotic activity when combined with each agonist as well as how stretch alters agonist-mediated protein secretion. We found that stretch contributed to overall fibrotic activity when added to individual agonists by either amplifying agonist-mediated downregulation or suppressing agonist-mediated upregulation of several matrix metalloproteinases. We further analyzed these data to identify cases in which stretch alters fibroblast sensitivity towards biochemical agonists and found that stretch sensitized fibroblasts towards agonists that downregulate protease expression and dampened the effects of agonist stimulation on protease upregulation. This systems-level study provides a resource of fibroblast protein expression in response to interacting environmental stimuli and highlights the complexity of intracellular signaling pathways in determining fibroblast phenotypes within the post-MI environment.

## Results

### mCF-seeded fibrin gels secrete matrix-regulating proteins across several orders of magnitude

In order to subject fibroblasts to biochemical stimuli and mechanical stretch, we used a multi-well stretching device in which deformable culture wells transmit uniaxial tension to 3-dimensional cell-seeded fibrin constructs suspended by opposite sets of vertical polydimethylsiloxane (PDMS) posts (Fig. 1A–B, see Materials and methods for full description). When subjected to uniaxial stretch within the culture wells, constructs experienced 6.5% axial strains with small, non-zero strains in the transverse direction, mimicking tissue strain patterns in the circumferential-longitudinal plane measured in rat and porcine infarct models [6,8,12,13]. mCFs maintained viability over a 96-h treatment period (Fig. S2) and aligned preferably towards the direction of stretch across all experimental groups (Fig. S3), which parallels previous studies that show preferential cell orientation towards both static boundary conditions and applied strain [14,15].

We used this culture platform to treat mCFs with either one of six biochemical agonists alone, cyclic stretch alone, or combinations of agonist treatments and stretch over a 96-h period to facilitate measurable protein secretion (Fig. 1C). Using a multiplexed immunoassay for simultaneous, quantitative detection of soluble proteins, we measured secreted levels of 13 secreted proteins associated with cardiac fibrosis in agonist−/stretch-treated samples (see Materials and methods for full description). Across all experimental groups, protein secretion varied across several orders of magnitude, from μM levels of collagen I-associated peptides to pM levels of several proteases and inhibitors (Fig. 2A). Interestingly, mCFs consistently expressed several species that have not been widely associated with fibroblast-specific protein expression, namely MMP12, TIMP4, and THBS4 [16]. Additionally, select proteins exhibit greater variance across experimental groups than others as evidenced by coefficients of variation (Fig. 2B), even within similar functional categories (e.g. MMP2/MMP9), which may be indicative of proteins with higher general sensitivity vs. robustness against stimulation.

### Biochemical stimuli differentially modulate secretion profiles of proteases and matricellular proteins

We examined the relationships between biochemical cues and fibrosis-related protein

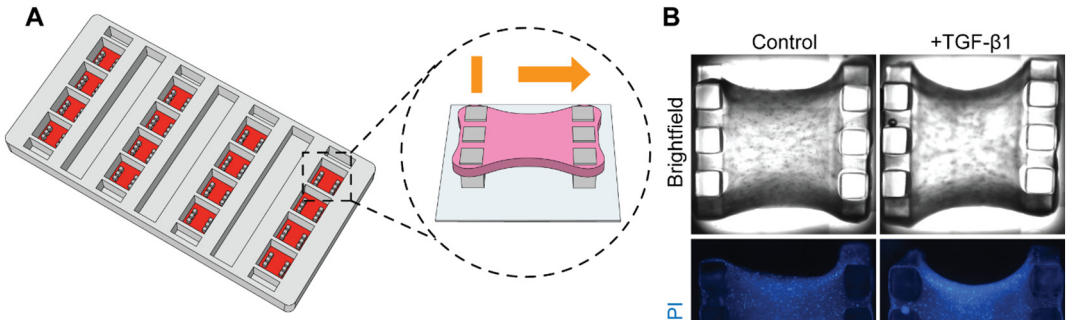


C

| | – Stretch | | + Stretch | |
|---|---|---|---|---|
| Agonist | LD (ng/mL) | HD (ng/mL) | LD (ng/mL) | HD (ng/mL) |
| Control | – | – | – | – |
| AngII | 1 | 100 | 1 | 100 |
| IL-1β | 10 | 1000 | 10 | 1000 |
| NE | 1 | 100 | 1 | 100 |
| PDGF | 1 | 100 | 1 | 100 |
| TGF-β1 | 10 | 1000 | 10 | 1000 |
| TNFα | 1 | 100 | 1 | 100 |

**Fig. 1.** Generation and treatment of cardiac fibroblast-seeded constructs. (A) Schematic of multi-well membrane modified with PDMS posts. Red surfaces represent silicone culture surfaces, with the addition and culture of cell-seeded fibrin resulting in anisotropic constructs that can be uniaxially stretched (cutout). (B) Brightfield (BF) and immunofluorescent staining for DAPI and αSMA for fibroblast-seeded gels after treatment. (C) Combinations of low dose (LD) and high dose (HD) biochemical agonists used in combination with cyclic stretch on fibroblast-seeded constructs. (For interpretation of the references to colour in this figure legend, the reader is referred to the web version of this article.)

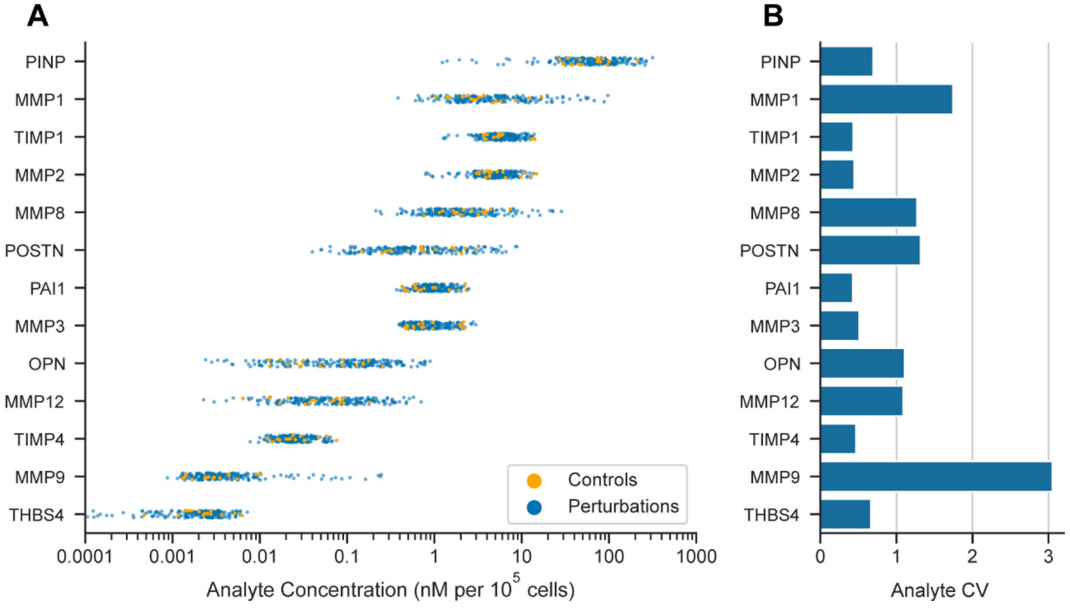


**Fig. 2.** Cardiac fibroblasts express fibrosis-regulating proteins across orders of magnitude in response to biochemical and mechanical perturbations. (A) Cell count-normalized protein concentrations for un-stretched controls and all perturbations (i.e. stretched, agonist-treated, or stretched and agonist-treated). (B) Coefficients of variation (CV) for protein concentrations across all conditions.

secretion by comparing the effects of biochemical agonists with un-stretched controls. Consistent with analyte coefficients of variation across all experimental groups, matricellular proteins POSTN and OPN and MMPs 1, 8, 9 and 12 were highly sensitive to biochemical stimulation with

variable expression across all treatment groups (Fig. 3A). Other species were robust to changes with biochemical cues resulting in minor trends with stimulation by TNFα and PDGF, including protease inhibitors, collagen I-associated peptides and MMPs 2 and 3. Across both sets of treatment doses, inflammatory cytokines IL-1β and TNFα uniquely regulated protein secretion compared to other agonist types, with high doses of both agonists particularly upregulating MMP9 secretion compared to unstretched controls ($p$=5.1E-4 and 3.9E-10 for IL-1β and TNFα respectively). Trending and significant increases in MMP1, MMP12, and collagen I-associated peptide levels additionally suggest that mCFs shift in balance towards the secretion of anti-fibrotic proteins in response to these inflammatory stimuli ($p$-values shown in Fig. S5A).

## Cyclic stretch combines with biochemical stimuli to dictate overall protein secretion

Although the importance of mechanotransduction in cardiac fibrosis has gained attention recently, it is still unclear how this signaling axis integrates with complex biochemical signaling during cardiac remodeling. We first examined cyclic stretch as an individual stimulus compared to un-stretched controls and found that stretched mCF cultures upregulated collagen I-associated peptide levels and showed trending increases in POSTN and MMPs 1, 8, and 12 compared to un-stretched controls (Fig. 3B, left column, $p$-values shown in Fig. S5B), indicating that stretch alone did not produce definitively pro-fibrotic behavior. We then examined the role of stretch in conjunction with biochemical signaling by comparing secreted protein levels for cultures subjected to agonist-stretch combinations to un-stretched controls. Like static cultures, matricellular proteins and MMPs 1, 8, 9 and 12 were the most variably secreted across agonists (Fig. 3B, right heatmap), although inflammatory cytokines showed notably weaker upregulation of MMPs 1, 9, and collagen I-associated peptides under stretch compared to static conditions.

In order to understand how mechanical stretch contributes to overall fibroblast-mediated remodeling, we quantified differences between the effects of agonist treatments alone (i.e. agonist-only treatments vs. un-stretched controls) and agonist-stretch combinations (i.e. combinations vs. un-stretched controls, see Materials and methods for full description). We categorized these differences in overall protein secretion into three groups: (1) stretch can have an *additive effect* by enhancing secretion levels beyond those of agonist stimulation alone (Fig. 4A with example in 4D), (2) stretch can have a *subtractive effect* by suppressing changes in secretion with agonist treatment (Fig. 4B with example in 4E), and (3) stretch can have an *inverting effect* by overriding the effect of agonist stimulation alone, thus changing the overall effect from upregulation to downregulation or vice versa (Fig. 4C with example in 4F). From this analysis, we found that stretch showed trending or significant additive effects on agonist stimulation for 11 agonist-secreted protein pairs and showed trending or significant antagonistic effects for 8 pairs.

Within the additive effect group, stretch showed the most evidence of further upregulating MMP12 (Fig. 4G), with increases in expression in conjunction with IL-1β ($p$=0.013 for agonist/stretch combination versus un-stretched controls), TNFα ($p$=0.023), NE ($p$=0.055), and AngII stimulation ($p$=0.12). Secreted levels of OPN were also further increased by stretch when combined with

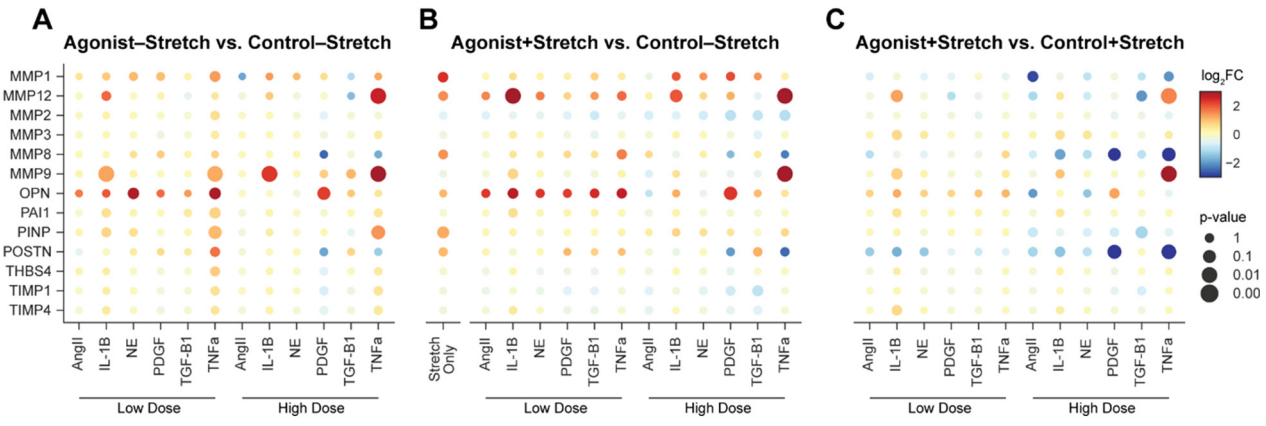


**Fig. 3.** Biochemical agonists and mechano-chemo combinations alter profiles of fibroblast secretion of matrix-related proteins. All values represent $\log_2$(fold-change) comparing each agonist treatment relative to designated controls. (A-C) Dot plots representing changes in secretion with individual agonists (A), changes in secretion with cyclic stretch (B), either alone (left column) or in combination with agonists, and changes in secretion with agonist-stretch in comparison to stretch-only samples (C). All statistical comparisons against respective controls were made using two-way ANOVA with Dunnett's post-hoc tests.

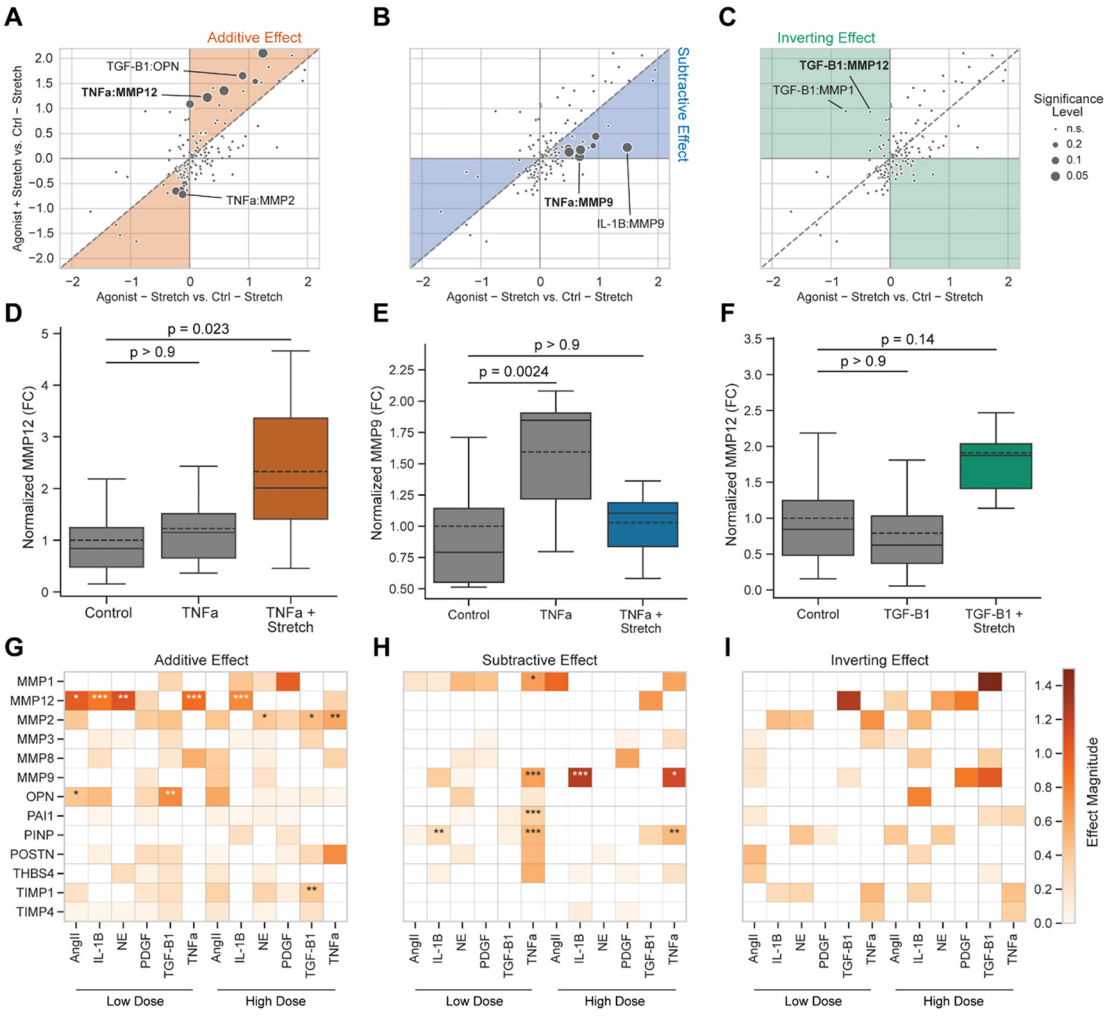


**Fig. 4.** Cyclic tension differentially alters the effects of biochemical stimulation on fibroblast protein secretion. (A-C) Effects of agonist-stretch combinations on overall protein secretion. X-coordinates represent the effect of agonist treatments alone relative to un-stretched controls, and y-coordinates represent the effect of agonist-stretch combinations relative to un-stretched controls. Shaded areas indicate secreted proteins that show an additive effect compared to agonist treatment alone (A), a subtractive effect (B), or an inverting effect from downregulation to upregulation and vice versa (C). (D-F) Representative plots demonstrating effects of agonist-stretch combinations compared to agonist treatment alone. Values for all groups are normalized to mean levels of un-stretched controls, solid lines represent median levels, dashed lines represent mean levels, and whiskers represent 1.5(IQR) levels. (G-I) Stretch effect magnitudes for cases of additive effect (G), subtractive effects (H), or inverting effects (I). Magnitudes are expressed in $\log_2$(fold-change), and Student's *t*-tests with Bonferroni correction for multiple comparisons are used for all comparisons against un-stretched controls. Asterisks represent level of confidence in interactions: * $p< 0.2$; ** $p< 0.1$; *** $p< 0.05$.

low-dose TGF-β1 and AngII treatments, resulting in approximately 3-fold increases relative to un-stretched controls ($p$=0.050 and 0.11, respectively). Stretch also showed synergistic trends in a suppressive manner; when combined with TNFα, TGF-β1, and NE treatments, stretch further decreased the expression of MMP2, leading to over 2-fold reductions in protease levels compared to un-stretched controls ($p$=0.10, 0.16, and 0.18, respectively). By quantifying differences between agonist-only effects and combination effects across all agonist-secreted protein pairs, we found that the addition of stretch exerts the largest changes in expression for MMP12, with multiple agonist/stretch combinations increasing secreted levels approximately 2-fold above agonist-only counterparts (Fig. 4G).

Stretch demonstrated subtractive effects on protein secretion by suppressing the secretion of matrix metalloproteinases that were upregulated by agonist treatments alone (Fig. 4B). MMP9 upregulation by several agonists was especially suppressed by stretch, as both IL-1β and TNFα significantly reduced expression in combination

with stretch compared to treatment with either cytokine alone (Fig. 4H). However, stretch also demonstrated antagonism towards the secretion of collagen I-associated peptides and protease inhibitor PAI1, as upregulated secretion of these species by IL-1β or TNFα were suppressed to near-control levels. Several agonist-secreted protein pairs also trended towards an inverting effect in which agonist/stretch combinations upregulated the expression of proteins that were downregulated by agonists alone (Fig. 4C), such as TGF-β1-mediated secretion of MMP12 (Fig. 4F). Although not meeting our criteria for statistical significance, these cases could also prove important in determining the full effect of stretch on cardiac remodeling, and further studies are necessary to explore these trends.

### Cyclic stretch modulates fibroblast sensitivity to biochemical stimulation

In order to quantify the ability of stretch to regulate biochemical signaling, we adapted the analysis discussed above to compare the effects of agonist treatments in a static context (i.e. agonist-only treatments vs. un-stretched controls) and in a stretched context (i.e. agonist/stretch combinations vs. stretch-only treatments). We categorized changes between contexts into three groups: (1) stretch can *sensitize* fibroblasts towards biochemical stimuli by enhancing the effect of agonist treatment under stretch (Fig. 5A, with example in 5D), (2) stretch can *desensitize* fibroblasts by suppressing the effect of agonist stimulation (Fig. 5B, with example in 5E), and (3) stretch can *reverse* fibroblast behavior completely by causing agonists to downregulate secretion compared to upregulation in a static environment, or vice versa (Fig. 5C, with example in 5F). We found that stretch showed evidence of agonist sensitization for 12 agonist-secreted protein pairs and showed similar evidence of agonist de-sensitization for 12 pairs compared to the same treatments under static conditions. None of the reversals were statistically significant.

Within the sensitizing group, stretch primarily acted to amplify agonist-mediated suppression, mediating further suppression of MMP8 levels by TNFα ($p$=0.044 for agonist/stretch combination versus stretched-only samples) and PDGF ($p$=0.059). Multiple agonists also exhibited amplified suppression of POSTN secretion with stretch, with TNFα, PDGF, and IL-1β all showing trending or significant suppression in a stretched context ($p$=0.020, 0.034, and 0.16 respectively). Interestingly, AngII appeared to further suppress MMP1, MMP12, and OPN under stretch, with MMP1 levels decreasing to almost 25% of those for stretch-only samples (Fig. 5D). Of these trends, secreted outputs MMP8 and POSTN appeared to have the highest degrees of sensitization, as TNFα and IL-1β reduced expression of these proteins by approximately 2.5-fold more under stretch than under static conditions (Fig. 5G).

Fibroblasts also showed decreases in sensitivity towards select agonist treatments under stretch (Fig. 5B); in particular, expression of MMP9 and OPN, both of which were upregulated in response to multiple agonists in static conditions, were not significantly altered by the same agonists under stretch (Fig. 5E). Interestingly, secretion of PINP and PAI1 also showed significant desensitization towards low-dose TNFα stimulation under stretch, although magnitudes of these changes were less than those for TNFα-mediated MMP9 secretion (Fig. 5H).

We additionally found that several agonist-secreted protein pairs demonstrated a reversal in sensitivity in which agonists that upregulated protein expression in static conditions downregulated expression under stretch (Fig. 5C). Like our findings of overriding effects described above, these cases did not meet our criteria for statistical significance. However, this type of behavior appears to be consistent for MMP1, MMP8, and POSTN expression (Fig. 5I), with TNFα stimulation reducing MMP1 expression to roughly 40% of stretch-only levels (Fig. 5F). Further studies validating these trends are necessary to fully understand the ability of stretch to reverse the effects of biochemical stimulation.

### Cyclic stretch differentially regulates global fibroblast sensitivity to cytokine stimulation

We lastly assessed the sensitivity of each secreted protein to all biochemical agonists in either static or stretched conditions to identify global trends in mechano-chemo interactions. Using a summed fold-change metric for total sensitivity, we found that matricellular proteins OPN and POSTN as well as MMPs 1, 8, 9, and 12 ranked as the most sensitive to biochemical treatment in both mechanical conditions (Fig. 6A). Within these outputs, OPN, MMP9, and MMP1 all showed de-sensitization towards all agonists under stretched conditions, although total sensitivity levels still ranked highly overall. Alternatively, both POSTN and MMP8 showed increased sensitivity to agonist stimulation in a high-stretch environment, indicating that these species may be more readily regulated within infarcted areas. Using a similar analysis to compare agonist regulation across all secreted outputs, we found that stretch altered the overall influence of TNFα, NE, and AngII on the secretion of all proteins (Fig. 6B). While stretch decreased the total magnitude of effects from TNFα stimulation, however, both NE and AngII exerted greater changes in protein levels within a stretched environment, more than doubling the influence of AngII on protein secretion.

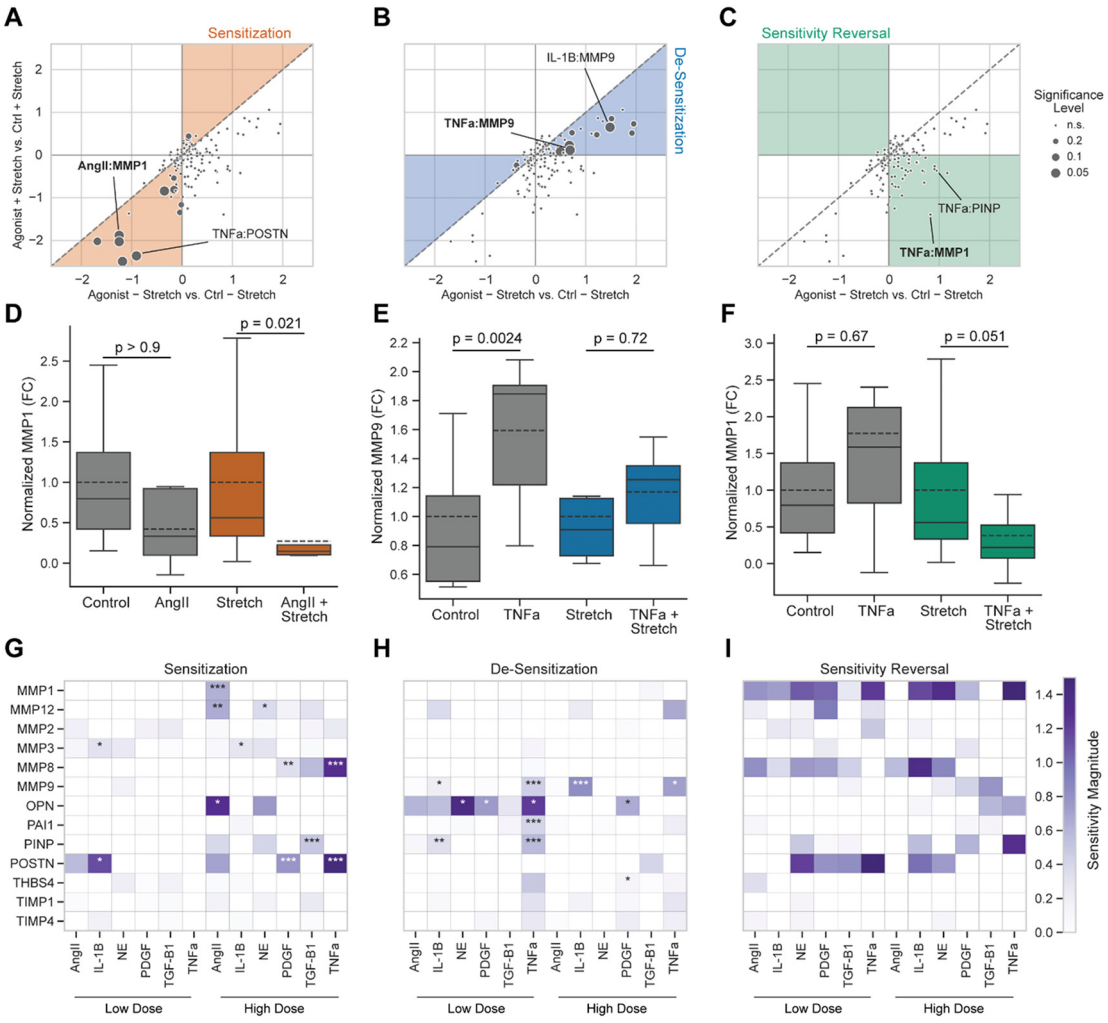


**Fig. 5.** Cyclic tension alters cardiac fibroblast sensitivity to biochemical agonists. (A-C) Changes in agonist effect on protein secretion for fibroblasts in static or strained cultures. X-coordinates represent effects of agonist treatments relative to un-stretched controls, and y-coordinates represent effects of agonist-stretch combinations relative to samples subjected to stretch only. Shaded areas indicate secreted proteins that show sensitization towards agonists (A), desensitization (B), or sensitivity reversal from upregulation to downregulation (C). (D-F) Representative plots demonstrating stretch-mediated changes in sensitivity of fibroblasts to agonist treatment. Values for un-stretched groups (gray) are normalized to mean levels of un-stretched controls, and values for stretched groups (colors) are normalized to mean levels of stretch-only groups. (G-I) Sensitivity magnitudes for cases of sensitization (G), desensitization (H), or sensitivity reversal (I). Magnitudes are expressed in $\log_2$(fold-change), and Student's *t*-tests with Bonferroni correction for multiple comparisons are used for all comparisons against respective controls. Asterisks represent level of confidence in interactions: * $p < 0.2$; ** $p < 0.1$; *** $p < 0.05$.

## Discussion

### Study design

The contribution of fibrosis to heart failure after MI has gained attention due to its role in chronic mechanical and electrical dysfunction. Prior studies of fibroblast behavior across many tissues and microenvironmental niches have highlighted the central role of dynamic mechanical stretch as well as biochemical signals in the regulation of diverse states of fibroblast activity [5,17,18]. By screening the effect of individual biochemical stimuli for their effects on fibroblast-specific matrix remodeling in the presence and absence of cyclic stretch, we sought to generate new insight into stretch-mediated fibrosis within the complex post-infarct environment. Future drug therapies that account for cell responses to this mechanical environment as well as responses to biochemical signals could improve patient outcomes.

In order to subject fibroblasts to biochemical stimuli and stretch while simulating myocardial architecture and material properties, we employed a previously developed strategy in which cells are incorporated into a fibrin matrix and seeded into

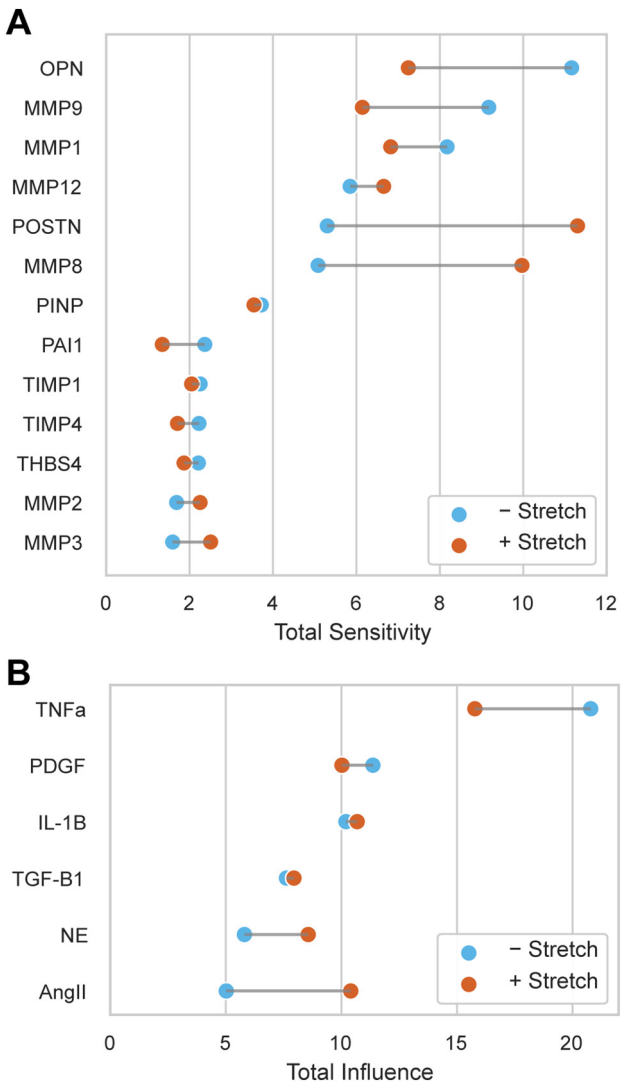


**Fig. 6.** Cyclic stretch modulates overall secretion of matrix-related proteins. (A) Sensitivity of individual secreted proteins to all biochemical agonists in both stretch contexts. Sensitivity levels for each output were calculated as the sum of $\log_2$(fold-change) values with each agonist relative to control as a representation of overall response of each output towards all agonists. (B) Influence of individual agonists across all secreted proteins in both stretch contexts. Values for respective analyses are ranked by un-stretched levels for each species. Influence levels for each agonist were calculated as the sum of $\log_2$(fold-change) values of each output relative to control as a representation of overall effect of each agonist towards all outputs.

culture wells containing vertical, opposing sets of silicone posts. Fibroblasts cultured in this manner have been shown to remodel the surrounding matrix and form aligned constructs with comparable stiffness to myocardial levels [19–22], thus mimicking in vivo mechanical conditions more closely than 2-dimensional mechanical testing systems which typically utilize culture surfaces with supraphysiologic stiffnesses. It should be noted that even upon returning to a soft substrate after culture on stiff substrates such as tissue culture plastic, fibroblasts permanently exhibit altered adhesion and maintain an activated state as reported by the Hinz group [23,24]. We acknowledge that this fundamental issue in mimicking in vivo conditions can confound mechanotransduction-related cell behavior. Although mCFs assumed an activated state throughout treatment, the use of soft gels prevented further stiffness-related stimulation during treatment, and myofibroblast-mediated remodeling could be examined without confounding mechanical factors.

## Relative secretion levels of matrix proteins and proteases

We first aimed to contextualize the effects of environmental cues on fibroblast-mediated scar formation by comparing absolute concentrations of mCFs-secreted proteins across and within

functional categories. Collagen I-associated peptides were predominately secreted along with MMP1, MMP2, MMP8, and TIMP1, which although secreted at distinct stages after myocardial injury [12], point to dominant mechanisms of ECM turnover via fibrillar collagen synthesis collagenase-mediated degradation. We also detected relatively small, but consistent levels of MMP12, TIMP4, and THBS4, all of which have been observed in fibroblast-specific gene expression studies but have not yet been directly measured at the protein expression level [16,25–27]. These biomarkers have been implicated in post-infarct remodeling either through paracrine signaling towards resolving inflammation as in the case of MMP12 [28], or by modulating responses to pressure overload as in the case of THBS4 [27]. Their direct link to cardiac fibroblast secretion suggests that fibroblasts may act in a communicatory role in addition to directly mediating matrix turnover.

### Differential sensitivity of secreted proteins and influence of biochemical stimuli

We compared fibroblast-specific matrix remodeling across biochemical stimuli by measuring matrix-related protein expression for six canonical agonists that have been shown to individually mediate fibroblast functional state through autocrine, paracrine, and hormonal signaling [5,29,30]. MMPs 1, 8, 9, and 12 and matricellular proteins OPN and POSTN were highly sensitive to agonist treatments compared to all other measured proteins. This finding of differential sensitivity towards stimuli is supported by targeted studies of MMP expression and activity such as that of Siwik and colleagues in which IL-1β treatment induced large increases in MMP9 activity relative to MMPs 2 and 13 [31]. Although absolute concentration levels were small for several proteins relative to other secreted outputs, large changes in expression suggest that select proteases may play an essential role in mediating biochemically driven matrix turnover.

Both inflammatory agonists used in our study exhibited a unique influence on protease expression relative to other agonists. We observed that both IL-1β and TNFα mediated significant increases in MMP9 levels, with TNFα additionally upregulating MMP12 expression, which suggest that inflammatory factors primarily acted to upregulate protease expression. These trends agree with parallel increases of inflammatory and protease levels within the acute post-infarct phase, which form the basis for removing necrotic tissue from the infarcted area [32–34], as well as in vivo studies in which TNFα$^{-/-}$ mice displayed reduced MMP9 expression, earlier collagen deposition, and reduced incidence of rupture post-MI compared to wild-type mice [35]. Both MMP9 and MMP12 have been implicated as key mediators of cardiac fibrosis and ventricular function post-MI, as MMP9$^{-/-}$ mice subjected to left coronary arterial ligation displayed enhanced MMP levels and attenuated collagen accumulation compared to wild-type mice [36], and Ramirez and colleagues found MMP9$^{-/-}$ mice exhibited improved responses to renin inhibitor aliskiren and angiotensin receptor inhibitor valsartan by attenuating increases in fibrotic gene expression, collagen content, and improving overall survival [37]. Pharmacological inhibition of MMP9 and MMP12 both exacerbated left ventricular function post-infarction [28,38], confirming the highly influential roles of both proteases and suggesting that MMP9-regulated tissue remodeling may be specific to the spatial and temporal context.

### Contribution of tension to overall protein secretion

Mechanical stretch has been widely shown to induce pro-fibrotic phenotypes in cardiac fibroblasts as one component of overall mechanical stimulation [39]. While previous work has shown that tensile forces can modulate fibroblast responses when combined with biochemical stimulation [10,11], it is still unclear how stretch contributes towards overall remodeling compared to biochemical signaling, and whether mechanical and biochemical signaling axes operate dependently or independently of each other. We aimed to answer these questions by treating mCF cultures with combinations of biochemical agonists and mechanical stretch and comparing the effects of these combinatory treatments to those of agonist-only treatments on protein expression.

We found that cyclic stretch altered protein secretion in two primary modalities: stretch either added to the effect of biochemical stimulation by further upregulating or suppressing protein secretion, or stretch subtracted from biochemically-mediated effects by suppressing expression levels to near-control levels. Stretch further increased expression of MMP12 and OPN compared to biochemical stimulation alone whereas secreted levels of MMP2 and MMP9 were downregulated, suggesting that stretch reinforces pro-fibrotic activity in fibroblasts by suppressing matrix proteases and increasing matricellular protein production. Although overall MMP levels are increased in the post-MI inflammatory phase with macrophages and neutrophils acting as the primary sources for secretion [16], our observed reductions in expression match a transition to the fibrotic phase involving the downregulation of MMPs and replacement of necrotic myocardium with collagenous scar [12]. MMP12 levels were uniquely amplified with stretch compared to cytokine treatment alone, which could be indicative of further negative feedback by MMP12 as knockdown studies in post-MI mice have shown both an increase in inflammatory signals in the myocardium and a decrease in beneficial remodeling [28,40]. Several recent studies have highlighted fibroblast phenotypic transitions

across inflammation, infiltration, proliferation, and fibrosis phases post-injury, with dynamic fibroblast expression patterns correlating to temporal variations in cytokine levels and cell functions [41–43]. Our new results also suggest a potential role for the dynamic post-MI mechanical context as a temporal mediator of these fibroblast transitions [8].

### Stretch-dependent sensitivity to biochemical stimulation

We additionally tested the hypothesis that stretch can not only act alongside biochemical stimuli but also alter cellular responses to these stimuli, as previous studies have demonstrated similar signaling mechanisms in both chemo- and mechano-transduction, such as mitogen-activated protein kinase and Akt signaling pathways [19,44–46]. We found that stretch altered fibroblast sensitivity towards agonists by either sensitizing cells towards agonists that suppress protease expression (e.g. MMP1, MMP8) or by de-sensitizing cells towards agonists that upregulate expression (e.g. MMP9). These changes in protease-related sensitivity indicate that stretch interacts with chemo-transduction pathways to selectively dampen matrix protease expression. While we also observed de-sensitization of both OPN and PINP upregulation towards biochemical stimuli under stretch, stretch alone upregulated the expression of both proteins, suggesting that these ECM components remained upregulated regardless of biochemical cues in a stretched environment. These results suggest that the underlying network of fibroblast signaling plays a large role in dictating fibroblast responses to competing cues, and further studies examining the intracellular signaling network are necessary to fully understand the mechanisms of action guiding fibroblast-mediated remodeling.

Our findings suggest that cardiac fibroblasts act in a mechano-adaptive manner to regulate matrix turnover, with mechanical stretch acting to alter matrix protease and matricellular protein secretion both directly, acting independently of biochemical signaling, and indirectly, acting to modify biochemical signaling. We found that TNFα-mediated protein secretion showed the highest degree of mechano-adaptive behavior compared to the other agonists tested, with stretch-mediated expression of MMP8, MMP9, MMP12, OPN, POSTN, PINP, and PAI1. Similar findings were recently found by Aguado and colleagues in which TNFα-mediated deactivation of cardiac fibroblasts was amplified depending on substrate stiffness, with a higher proportion of cells reverting towards quiescence on stiff hydrogels [47]. Our evidence of stretch-mediated sensitization and de-sensitization towards TNFα suggests that TNFα signaling mediates fibroblast activation under dynamic mechanical conditions. Further studies are necessary to validate these relationships between inflammation and stretch in guiding fibroblast phenotypes.

### Study limitations and future directions

One limitation of this study arises from the variability that arises from the measurement of protein expression across biological replicates. The use of separate pools of mCFs in our comparisons allowed for genomic variability between replicates, and although our use of a mixed-effect statistical model was able to discern agonist- and stretch-mediated behavior, we cannot rule out additional mechano-chemo interactions that we were unable to detect. However, the interactions that we identified in our analysis persisted despite this variability, thereby improving our confidence in these findings. Our screen of mechano-chemo interactions was additionally limited to two doses of biochemical stimulation and two mechanical states, and further dose-response studies would further explore the extent of relationships between these stimuli. Additionally, a number of other secreted factors were not measured in our study that have been shown to play significant roles in matrix remodeling, including those related to matrix processing and turnover (e.g. cathepsins, lysyl oxidase, etc.) and paracrine signaling (e.g. tenascin-c, interleukins, thrombospondins, etc.). Further measurements would provide insight into the contribution of fibroblast secretion towards maladaptive remodeling.

Lastly, our data suggest that fibroblast secretion relies on a complex network of intracellular signaling, which contains interactions between transduction pathways that dictate overall responses. Several groups have successfully identified influential mechanisms of mechano-transduction and mechano-chemo crosstalk using computational models of cell signaling [42,48–52], providing new directions towards controlling cell behavior in a dynamic mechanical environment. For translation of these model predictions to tissue-scale remodeling and clinical use however, proteomic datasets containing fully-quantified information for protein states (i.e. absolute active/total protein concentrations) are critical for transforming semi-quantitative systems models into those capable of predicting absolute changes in cell and tissue properties. The quantitative nature of this current proteomic dataset presents opportunities for fitting systems-level models to quantitative data and allows for quantitative predictions of fibroblast secretion, and future work integrating these models with proteomic datasets are necessary to predict fibroblast-mediated matrix remodeling on a systems level.

## Conclusions

We developed a screen of cardiac fibroblast protein secretion in response to combinations of biochemical agonists and mechanical stretch to investigate how cyclic stretch influences fibrotic activity within the context of biochemical signaling.

We found that biochemical stimuli primarily altered the expression of MMPs 1, 8, 9, 12, OPN, and POSTN, and inflammatory agonists IL-1β and TNFα particularly promoted protease secretion, thereby shifting the balance in matrix turnover towards degradation. The addition of stretch to biochemical stimuli shifted fibroblast behavior towards matrix accumulation by either further upregulating matricellular protein expression, further downregulating protease expression, or antagonizing the upregulation of MMP9 by inflammatory agonists. We also found that stretch mediated fibroblast sensitivity towards biochemical stimuli by increasing sensitivity towards agonists that suppress MMP1, MMP8, and POSTN while decreasing sensitivity towards those that upregulate MMP9, thereby priming cells towards matrix accumulation. The screening approach employed here allows for the identification of emergent interactions between cell stimuli and can be used to inform targeted studies for interactions that govern matrix turnover.

## Materials and methods

### Cardiac fibroblast isolation

All animal procedures were conducted in accordance with the Institutional Animal Care and Use Committee at Clemson University. mCFs were isolated and cultured as previously reported [53]. Wild-type C57BL/6 mice (male, 10–12 weeks old, ~25 g body weight) were sacrificed, and hearts were harvested and collected in Krebs-Henseleit buffer (Sigma, St. Louis, MO). The ventricles were isolated, minced, and digested enzymatically at 37 °C with Liberase TM (Roche, Indianapolis, IN). Supernatants from six successive digestion periods were collected, centrifuged at 300 × *g* at 4 °C, and resuspended into Dulbecco's Modified Eagle's Medium (DMEM, Sigma) containing 10% fetal bovine serum (FBS, Atlanta Biologicals, Flowery Branch, GA), 100 U/mL penicillin G, 100 μg/mL streptomycin, and 1 ng/mL amphotericin B (all Sigma). Cells were plated in culture flasks and incubated at 37 °C and 5% $CO_2$ for 4 h. Fresh culture medium was added to remove non-adherent cells, and culture medium was replaced every 48 h thereafter. mCFs were cultured on tissue culture plastic until passage 2 before seeding in fibrin gels as described below.

### Fibroblast-seeded fibrin gels

mCFs were seeded into fibrin gels using a previously reported procedure [21] and loaded gels into silicone 16-well plates (CellScale, Waterloo, ON). Fibrin was chosen as a scaffold material for its ability to promote de novo collagen synthesis and fibroblast-mediated remodeling. Previous studies embedding human dermal fibroblasts and smooth muscle cells in fibrin gels have demonstrated improved synthesis of collagen compared to collagen gels, which tend to inhibit synthesis [54–56]. Fibrin additionally allows for cell-initiated remodeling and compaction of the matrix for a functional assessment of cell contractility, and cell-remodeled fibrin gels of a similar density as those used here have been shown to have a linear modulus of 19–28 kPa [57], which is more comparable to the stiffness of healthy myocardium (10–25 kPa) [39] than collagen gels of a similar density [57]. Fibrin has been the focus of tissue regeneration strategies post-MI as a scaffold for cell transplantation [58] with cell-seeded fibrin injected into the myocardium improving post-MI function in mice [59], and thus the study of fibroblast-mediated remodeling and secretion within this matrix could also prove useful for tissue engineering applications.

Prior to plating gels, well plates were modified to contain six PDMS posts each, which have been shown to facilitate gel remodeling by fibroblasts [20,21,60,61]. To construct the posts, a Delrin mold was fabricated via milling with a negative pattern for sets of three posts corresponding with axial ends of each construct. Individual post geometries were 1 mm × 1 mm × 2 mm (l x w x h), and posts were spaced 0.75 mm apart within each pattern. Upon fabrication of the negative mold, Sylgard 184 PDMS (Dow Corning, Midland, MI) was mixed at a 10:1 ratio (base: curing agent), poured into the mold, degassed via a vacuum desiccator for 10 min, and cured in a 95 °C oven for 1 h to allow for polymerization for an elastic modulus of approximately 700 kPa as determined by previous studies [62]. Upon curing, sets of posts were removed from the mold and bonded to 16-well plates using freshly mixed Sylgard 184 PDMS as a glue. Two sets of posts were placed in each well and spaced 5 mm apart on opposing sides in the direction of stretch. Well plates were then placed in a 95 °C oven for 1 h to allow for polymerization of the PDMS glue. Prior to use, wells were additionally coated with 3.5% Pluronic F-127 (Sigma) in phosphate buffered saline (PBS, Sigma) for 8 min to prevent adhesion to the well surfaces.

Upon well plate modification, mCFs were removed from flasks with 0.25% Trypsin-EDTA (Gibco, Grand Island, NY) and incubated with DiI (Invitrogen, Grand Island, NY) to visualize cell membranes after treatment. Cells were resuspended in a thrombin solution (0.44 U/mL bovine thrombin in DMEM with 0.5% FBS) and combined with a fibrinogen solution (6.6 mg/mL in 20 mM HEPES-buffered saline) at a 1:1 ratio to create a fibrin gel. Upon combining, 200 uL of fibrin gel was added to each well, and gels were incubated at 37 °C for 30 min to allow for polymerization. DMEM containing 0.5% FBS, 50 μg/mL L-ascorbic acid (Sigma), and 33.3 μg/mL aprotinin (Roche) was then added to each well to prevent premature degradation of fibrin gels. Although a well-known inhibitor of MMP activation, the expression of collagens, proMMPs, and gel contraction compared to negative controls have been shown to remain unchanged with added

aprotinin in fibroblast- and mesenchymal stromal cell-seeded gels [63,64], suggesting that this inhibitor allows for the measurement of protease and matrix secretion while maintaining structural integrity of fibrin constructs. After addition of this culture medium, gels were cultured for 48 h to allow for gel remodeling. For each replicate, 14 gels were seeded with $1 \times 10^5$ mCFs for compaction, viability, and immunocytochemistry analyses, and 14 gels were seeded with $2 \times 10^5$ mCFs to collect sufficient protein for secretomic analysis.

### Cyclic stretch and cytokine treatment

Prepared well plates were loaded into MechanoCulture FX2 uniaxial stretching devices (CellScale, Waterloo, ON). For stretched gels, a strain amplitude of 6.5% and frequency of 1.0 Hz was used, which were chosen to match typical strain patterns measured in a variety of animal models including acute cryoinfarction and permanent coronary artery ligation in rats and pigs [6,8,12,13]. Axial and transverse strains for gels were validated by measuring gel deformation during 0.33-mm increments of stretch by the device actuator and calculating the 1,1 (axial) and 2,2 (transverse) components of the Green strain tensor from each set of values (Fig. S1). Gels within each stretch condition were treated with either no agonist (control group) or one of six cytokines or growth factors: transforming growth factor-β1 (TGF-β1, Cell Signaling Technology, Danvers, MA), angiotensin II (AngII, Sigma), interleukin-1β (IL-1β, Cell Signaling Technology), platelet-derived growth factor-BB (PDGF, Cell Signaling Technology), L-norepinephrine bitartrate (NE, Sigma), and tumor necrosis factor-α (TNFα, Cell Signaling Technology). These agonists have all been shown to influence fibrotic remodeling post-MI at both tissue and cellular scales [65]; AngII and NE, both canonical mediators of cardiac hypertrophy, have been shown to alter fibroblast-specific remodeling, with in vivo and in vitro studies of angiotensin receptor blockers and neprilysin inhibitors attenuating fibrosis caused by AngII infusion [66,67]. TGF-β1 and PDGF as growth factors have also become well-known mediators of fibroblast activation and fibrosis both post-MI and systemically [68–70], and inhibition of either factor has been shown to attenuate fibrosis in the infarcted myocardium [69,71]. Inflammatory agonists IL-1β and TNFα additionally alter cardiac fibrosis as shown in clinical trials of IL-1β inhibitor anakinra and animal studies overexpressing TNFα [72,73]. While not an exhaustive study of possible fibroblast agonists, these six agonists represent several major modes of fibroblast activation post-MI. All concentrations were chosen from previous literature measuring fibroblast responses to individual agonists including collagen expression [50,74–76], MMP, TIMP, and growth factor expression [75,77], and αSMA expression or gel contraction [50] (concentrations displayed in Fig. 1C). All gels were treated for a total of 96 h, during which doses and medium were replenished after 48 h.

### Gel compaction analysis

Brightfield images were taken at the beginning and end of treatment using an EVOS FL Auto microscope with a 4× Plan Fluor 0.13 NA objective (Life Technologies, Grand Island, NY). A $4 \times 3$ grid of images were captured and combined to create a composite image of each gel. Gel outlines were then segmented using the threshold feature in ImageJ [78]. Gel compaction was calculated as the fold change of the final gel area from the initial gel area.

### Immunocytochemistry and image analysis

Cell viability was determined via a fluorescence-based assay as described previously [79]. Gels were stained using a live/dead cell double staining kit (Sigma) according to the manufacturer instructions, and fluorescent images were captured at the center of each gel for calcein and propidium iodide to identify viable and dead cells, respectively. CellProfiler software was used for quantitative image analysis [80]. Viable cells were identified from calcein images using a minimum cross entropy thresholding method, and dead cells were identified from propidium iodide images using a manual threshold to remove false positives due to low numbers of dead cells per image. Cell viability for each gel was determined as the ratio of viable cells to total cells, and cell orientation was measured for viable cells as the angle from the axis of stretch to the major axis of each cell.

For analysis of fibroblast activation, immunostaining and quantitative analysis were performed as reported previously [50]. Gels were fixed in 10% neutral buffered formalin (VWR, Radnor, PA) and washed 3× in PBS. Gels were permeabilized in 0.2% Triton-X-100 (Sigma) in PBS and washed 3× in PBS, and gels were blocked with 2% bovine serum albumin (Sigma) at 4 °C overnight. Gels were stained with alpha smooth muscle actin-Alexa Fluor 488 (αSMA, Invitrogen) and 4′,6-diamidino-2-phenylindole, dihydrochloride (DAPI, Invitrogen), washing gels 3× with PBS after applying each stain. Fluorescent images were captured at the center of each gel for DAPI, αSMA, and DiI stains. Using CellProfiler software, individual cells were identified by DAPI and DiI stains, and integrated αSMA intensity was measured within each identified cell. Mean αSMA expression levels were calculated as the average integrated intensities across all cells per image. Total cell counts for each gel were extrapolated using final gel areas calculated in compaction analysis (Fig. S4A). From the number of identified cells in each image, total cell counts for each gel were calculated as the product of the cell density in each image and the final gel area.

### Secreted protein measurement

During cell treatments, culture supernatants were collected at both 48 h and 96 h after initial treatment and stored at −20 °C. Pro-collagen I amino-terminal propeptide (PINP) and matrix metalloproteinase-1 (MMP1) content were both measured via enzyme-linked immunosorbent assay as per the manufacturer's instructions (MyBiosource, San Diego, CA). Luminex magnetic bead assays (R&D Systems, Minneapolis, MN) were used to measure a panel of 11 additional analytes: MMP2, 3, 8, 9, and 12, tissue inhibitors of matrix metalloproteinases-1 and 4 (TIMP1 and 4), osteopontin (OPN), periostin (POSTN), thrombospondin-4 (THBS4), and plasminogen activator inhibitor-1 (PAI1). These analytes were chosen as representatives known to influence cardiac fibrosis via matrix production, degradation, or further signaling mechanisms involving fibroblasts or other cell types, and have been implicated as clinically-relevant soluble markers of scar formation [81]. In addition to direct synthesis of matrix proteins as measured by PINP levels and secretion of matrix-degrading proteins as measured by MMP levels, matricellular proteins POSTN, OPN, and THBS4 have been shown to mediate fibrosis in pressure overload models by as in the case of OPN and THBS4 [27,82], or in fibroblast-specific ablation post-MI as in the case of POSTN [83,84], suggesting possible sensitivity towards mechanical stress as well as prominent roles in matrix turnover. Therefore, we included these outputs to provide a representative dataset of mechano-chemo interactions that encompasses multiple fibrosis-related processes in addition to the secretion of matrix proteins and proteases. Luminex assays were measured using a MAGPIX magnetic bead reader (Luminex, Austin, TX). Absolute protein concentrations were determined from standard curves for each analyte, and all concentrations were normalized by total cell counts as determined above to account for proliferation-related bias.

### Agonist-stretch effect analysis

For each measured protein, contrasts between two sets of experimental groups were assessed: (i) agonist treatments alone and controls ($\Delta T_0$), and (ii) combined agonist-stretch treatments and controls ($\Delta TS$). Contrasts for both sets were expressed as $\log_2$(fold change), and effect magnitudes were calculated as change between contrasts: $E_m = |\Delta TS - \Delta T_0|$. Effect directions were calculated as the difference between contrast magnitudes: $E_d = |\Delta TS| - |\Delta T_0|$. Signs of effect direction terms were used to determine categories of combinatorial effects: a positive term denoted an additive effect of combined treatment (i.e. stretch further increased or decreased protein secretion beyond agonist treatment alone), and a negative term denoted a subtractive effect (i.e. stretch suppressed the effect of agonist treatment alone). Individual contrasts that had opposite signs (e.g. $\Delta T_0<0$ and $\Delta TS>0$) were denoted as inverting effects.

### Agonist-stretch sensitivity analysis

In a similar manner to effect analysis above, contrasts between two sets of experimental groups were assessed: (i) agonist treatments alone and controls ($\Delta T_0$), and (ii) combined agonist-stretch treatments and samples subjected to stretch only ($\Delta T_s$). Contrasts for both sets were expressed as $\log_2$(fold change), and sensitivity magnitudes were calculated as the change between contrasts: $S_m = |\Delta T_s - \Delta T_0|$. Sensitivity directions were calculated as the difference between contrast magnitudes: $S_d = |\Delta T_s| - |\Delta T_0|$. Signs of sensitivity direction terms were similarly used to determine categories of sensitivity changes: a positive term denoted a sensitizing effect of stretch on agonist treatment (i.e. stretch caused a greater response to agonist stimulation), and a negative term denoted a de-sensitizing effect (i.e. stretch caused a dampened response to agonist stimulation). Individual contrasts that had opposite signs (e.g. $\Delta T_0<0$ and $\Delta T_s>0$) were denoted as reversal effects.

### Statistical analysis

Statistical analyses were performed using the lme4 package in the R statistical suite [85]. mCFs were isolated from 8 groups of mice representing one biological replicate each, and cells were equally divided between all experimental groups within each replicate for $N$=8 replicates per experimental group. For each measured protein, normalized concentrations were fit to a linear mixed-effect model in which biochemical agonists and stretch states were modeled as fixed variables, and biological replicate was modeled as a random variable. Analysis of deviance was used to assess the model validity in comparison to a null model containing only random variables, using a type I error rate of 0.05 for valid models. Two-factor ANOVA was used to test fixed variables, Dunnett's post-hoc tests were used for multiple comparisons between agonists and respective controls, and Student's $t$-tests with Bonferroni correction were used for individual comparisons made in agonist-stretch effect and sensitivity analyses.

## Funding

This study was supported by the National Institutes of Health (GM121342, GM103444, HL144927) and the American Heart Association (17SDG33410658).

## Disclosures

None.

## DECLARATION OF COMPETING INTEREST

The authors declare that they have no known competing financial interests or personal relationships that could have appeared to influence the work reported in this paper.


### Acknowledgements

We thank Joseph Bible Ph.D. for his assistance in developing the statistical model used in this study, and the Godley-Snell Research Center for assisting in cardiac fibroblast isolation.


## Appendix A. Supplementary data

Supplementary data to this article can be found online at https://doi.org/10.1016/j.mbplus.2020.100055.


*Received 5 September 2020;*
*Accepted 23 November 2020;*
*Available online 30 December 2020*

***Keywords***:
Cardiac fibroblast;
Mechanotransduction;
Fibrosis;
Signaling interactions;
ECM


## References


[1]. Benjamin, E.J., Blaha, M.J., Chiuve, S.E., Cushman, M., Das, S.R., Deo, R., de Ferranti, S.D., Floyd, J., Fornage, M., Gillespie, C., Isasi, C.R., Jiménez, M.C., Jordan, L.C., Judd, S.E., Lackland, D., Lichtman, J.H., Lisabeth, L., Liu, S., Longenecker, C.T., Mackey, R.H., Matsushita, K., Mozaffarian, D., Mussolino, M.E., Nasir, K., Neumar, R. W., Palaniappan, L., Pandey, D.K., Thiagarajan, R.R., Reeves, M.J., Ritchey, M., Rodriguez, C.J., Roth, G.A., Rosamond, W.D., Sasson, C., Towfighi, A., Tsao, C.W., Turner, M.B., Virani, S.S., Voeks, J.H., Willey, J.Z., Wilkins, J.T., Wu, J.H., Alger, H.M., Wong, S.S., Muntner, P., (2017). Heart disease and stroke statistics—2017 update: a report from the American Heart Association. *Circulation*, **135**, e146–e603. https://doi.org/10.1161/CIR.0000000000000485.

[2]. Puymirat, E., Simon, T., Cayla, G., Cottin, Y., Elbaz, M., Coste, P., Lemesle, G., Motreff, P., Popovic, B., Khalife, K., Labèque, J.-N., Perret, T., Le Ray, C., Orion, L., Jouve, B., Blanchard, D., Peycher, P., Silvain, J., Steg, P. G., Goldstein, P., Guéret, P., Belle, L., Aissaoui, N., Ferrières, J., Schiele, F., Danchin, N., (2017). Acute myocardial infarction: changes in patient characteristics, management, and 6-month outcomes over a period of 20 years in the FAST-MI Program (French Registry of Acute ST-Elevation or Non-ST-Elevation Myocardial Infarction) 1995 to 2015. *Circulation*, **136**, 1908–1919. https://doi.org/10.1161/CIRCULATIONAHA.117.030798.

[3]. Verluyten, M.J.A., Smits, J.F.M., Daemen, M.J.A.P., (1995). Collagen remodeling after myocardial infarction in the rat heart. *Am. J. Pathol.*, **147**, 325–338.

[4]. Chen, W., Frangogiannis, N.G., (2013). Fibroblasts in post-infarction inflammation and cardiac repair. *Biochim. Biophys. Acta, Mol. Cell Res.*, **1833**, 945–953. https://doi.org/10.1016/j.bbamcr.2012.08.023.

[5]. Bretherton, R., Bugg, D., Olszewski, E., Davis, J., (2020). Regulators of cardiac fibroblast cell state. *Matrix Biol.*, **91–92**, 117–135. https://doi.org/10.1016/j.matbio.2020.04.002.

[6]. Fomovsky, G.M., Rouillard, A.D., Holmes, J.W., (2012). Regional mechanics determine collagen fiber structure in healing myocardial infarcts. *J. Mol. Cell. Cardiol.*, **52**, 1083–1090. https://doi.org/10.1016/j.yjmcc.2012.02.012.

[7]. Torres, W.M., Jacobs, J., Doviak, H., Barlow, S.C., Zile, M.R., Shazly, T., Spinale, F.G., (2018). Regional and temporal changes in left ventricular strain and stiffness in a porcine model of myocardial infarction. *Am. J. Physiol. Circ. Physiol.*, **315**, H958–H967. https://doi.org/10.1152/ajpheart.00279.2018.

[8]. Fomovsky, G.M., Holmes, J.W., (2010). Evolution of scar structure, mechanics, and ventricular function after myocardial infarction in the rat. *Am. J. Physiol. Heart Circ. Physiol.*, **298**, H221–H228. https://doi.org/10.1152/ajpheart.00495.2009.

[9]. Herum, K.M., Lunde, I.G., Mcculloch, A.D., Christensen, G., (2017). The soft- and hard-heartedness of cardiac fibroblasts: mechanotransduction signaling pathways in fibrosis of the heart. *J. Clin. Med.*, **6** (5), 53. https://doi.org/10.3390/jcm6050053.

[10]. Lindahl, G.E., Chambers, R.C., Papakrivopoulou, J., Dawson, S.J., Jacobsen, M.C., Bishop, J.E., Laurent, G. J., (2002). Activation of fibroblast procollagen 1(I) transcription by mechanical strain is transforming growth factor- -dependent and involves increased binding of CCAAT-binding factor (CBF/NF-Y) at the proximal promoter. *J. Biol. Chem.*, **277**, 6153–6161. https://doi.org/10.1074/jbc.M108966200.

[11]. Merryman, W.D., Lukoff, H.D., Long, R.A., Engelmayr, G. C., Hopkins, R.A., Sacks, M.S., (2007). Synergistic effects of cyclic tension and transforming growth factor-β1 on the aortic valve myofibroblast. *Cardiovasc. Pathol.*, **16**, 268–276. https://doi.org/10.1016/J.CARPATH.2007.03.006.

[12]. Richardson, W.J., Clarke, S.A., Quinn, T.A., Holmes, J. W., (2015). Physiological implications of myocardial scar structure. *Compr. Physiol.*, **5**, 1877–1909. https://doi.org/10.1002/cphy.c140067.

[13]. Holmes, J.W., Yamashita, H., Waldman, L.K., Covell, J. W., (1994). Scar remodeling and transmural deformation after infarction in the pig. *Circulation.*, **90**, 411–420. https://doi.org/10.1161/01.CIR.90.1.411.

[14]. Pang, Y., Wang, X., Lee, D., Greisler, H.P., (2011). Dynamic quantitative visualization of single cell alignment and migration and matrix remodeling in 3-D collagen hydrogels under mechanical force. *Biomaterials.*, **32**, 3776–3783. https://doi.org/10.1016/j.biomaterials.2011.02.003.

[15]. Chen, K., Vigliotti, A., Bacca, M., McMeeking, R.M., Deshpande, V.S., Holmes, J.W., (2018). Role of boundary conditions in determining cell alignment in response to stretch. *Proc. Natl. Acad. Sci. U. S. A.*, **115**, 986–991. https://doi.org/10.1073/pnas.1715059115.

[16]. Lindsey, M.L., Zamilpa, R., (2012). Temporal and spatial expression of matrix metalloproteinases and tissue inhibitors of metalloproteinases following myocardial infarction. *Cardiovasc. Ther.*, **30**, 31–41. https://doi.org/10.1111/j.1755-5922.2010.00207.x.

[17]. Soliman, H., Rossi, F.M.V., (2020). Cardiac fibroblast diversity in health and disease. *Matrix Biol.*, **91–92**, 75–91. https://doi.org/10.1016/j.matbio.2020.05.003.

[18]. DeLeon-Pennell, K.Y., Barker, T.H., Lindsey, M.L., (2020). Fibroblasts: the arbiters of extracellular matrix remodeling. *Matrix Biol.*, **91–92**, 1–7. https://doi.org/10.1016/j.matbio.2020.05.006.

[19]. Schmidt, J.B., Chen, K., Tranquillo, R.T., (2016). Effects of intermittent and incremental cyclic stretch on ERK signaling and collagen production in engineered tissue. *Cell. Mol. Bioeng.*, **9**, 55–64. https://doi.org/10.1007/s12195-015-0415-6.

[20]. Legant, W.R., Pathak, A., Yang, M.T., Deshpande, V.S., McMeeking, R.M., Chen, C.S., (2009). Microfabricated tissue gauges to measure and manipulate forces from 3D microtissues. *Proc. Natl. Acad. Sci.*, **106**, 10097–10102. https://doi.org/10.1073/pnas.0900174106.

[21]. Kural, M.H., Billiar, K.L., (2016). Myofibroblast persistence with real-time changes in boundary stiffness. *Acta Biomater.*, **32**, 223–230. https://doi.org/10.1016/j.actbio.2015.12.031.

[22]. Duong, H., Wu, B., Tawil, B., (2009). Modulation of 3D fibrin matrix stiffness by intrinsic fibrinogen–thrombin compositions and by extrinsic cellular activity. *Tissue Eng. Part A.*, **15**, 1865–1876. https://doi.org/10.1089/ten.tea.2008.0319.

[23]. Balestrini, J.L., Chaudhry, S., Sarrazy, V., Koehler, A., Hinz, B., (2012). The mechanical memory of lung myofibroblasts. *Integr. Biol.*, **4**, 410–421. https://doi.org/10.1039/c2ib00149g.

[24]. Li, C.X., Talele, N.P., Boo, S., Koehler, A., Knee-Walden, E., Balestrini, J.L., Speight, P., Kapus, A., Hinz, B., (2017). MicroRNA-21 preserves the fibrotic mechanical memory of mesenchymal stem cells. *Nat. Mater.*, **16**, 379–389. https://doi.org/10.1038/nmat4780.

[25]. Mouton, A.J., Ma, Y., Rivera Gonzalez, O.J., Daseke, M. J., Flynn, E.R., Freeman, T.C., Garrett, M.R., DeLeon-Pennell, K.Y., Lindsey, M.L., (2019). Fibroblast polarization over the myocardial infarction time continuum shifts roles from inflammation to angiogenesis. *Basic Res. Cardiol.*, **114**, 6. https://doi.org/10.1007/s00395-019-0715-4.

[26]. Quaife-Ryan, G.A., Sim, C.B., Ziemann, M., Kaspi, A., Rafehi, H., Ramialison, M., El-Osta, A., Hudson, J.E., Porrello, E.R., (2017). Multicellular transcriptional analysis of mammalian heart regeneration. *Circulation.*, **136**, 1123–1139. https://doi.org/10.1161/CIRCULATIONAHA.117.028252.

[27]. Frolova, E.G., Sopko, N., Blech, L., Popović, Z.B., Li, J., Vasanji, A., Drumm, C., Krukovets, I., Jain, M.K., Penn, M.S., Plow, E.F., Stenina, O.I., (2012). Thrombospondin-4 regulates fibrosis and remodeling of the myocardium in response to pressure overload. *FASEB J.*, **26**, 2363–2373. https://doi.org/10.1096/fj.11-190728.

[28]. Iyer, R.P., Patterson, N.L., Zouein, F.A., Ma, Y., Dive, V., de Castro Brás, L.E., Lindsey, M.L., (2015). Early matrix metalloproteinase-12 inhibition worsens post-myocardial infarction cardiac dysfunction by delaying inflammation resolution. *Int. J. Cardiol.*, **185**, 198–208. https://doi.org/10.1016/j.ijcard.2015.03.054.

[29]. Deschamps, A., Spinale, F., (2006). Pathways of matrix metalloproteinase induction in heart failure: bioactive molecules and transcriptional regulation. *Cardiovasc. Res.*, **69**, 666–676. https://doi.org/10.1016/j.cardiores.2005.10.004.

[30]. Bradshaw, A.D., DeLeon-Pennell, K.Y., (2020). T-cell regulation of fibroblasts and cardiac fibrosis. *Matrix Biol.*, **91–92**, 167–175. https://doi.org/10.1016/j.matbio.2020.04.001.

[31]. Siwik, D.A., Chang, D.L.F., Colucci, W.S., (2000). Interleukin-1 β and tumor necrosis factor-α decrease collagen synthesis and increase matrix metalloproteinase activity in cardiac fibroblasts in vitro. *Circ. Res.*, **86**, 1259–1265. https://doi.org/10.1161/01.RES.86.12.1259.

[32]. Ono, K., Matsumori, A., Shioi, T., Furukawa, Y., Sasayama, S., (1998). Cytokine gene expression after myocardial infarction in rat hearts. *Circulation.*, **98**, 149–156. https://doi.org/10.1161/01.CIR.98.2.149.

[33]. LaFramboise, W.A., Bombach, K.L., Dhir, R.J., Muha, N., Cullen, R.F., Pogozelski, A.R., Turk, D., George, J.D., Guthrie, R.D., Magovern, J.A., (2005). Molecular dynamics of the compensatory response to myocardial infarct. *J. Mol. Cell. Cardiol.*, **38**, 103–117. https://doi.org/10.1016/J.YJMCC.2004.09.011.

[34]. Etoh, T., Joffs, C., Deschamps, A.M., Davis, J., Dowdy, K., Hendrick, J., Baicu, S., Mukherjee, R., Manhaini, M., Spinale, F.G., (2001). Myocardial and interstitial matrix metalloproteinase activity after acute myocardial infarction in pigs. *Am. J. Physiol. Circ. Physiol.*, **281**, H987–H994. https://doi.org/10.1152/ajpheart.2001.281.3.H987.

[35]. Sun, M., Dawood, F., Wen, W.H., Chen, M., Dixon, I., Kirshenbaum, L.A., Liu, P.P., (2004). Excessive tumor necrosis factor activation after infarction contributes to susceptibility of myocardial rupture and left ventricular dysfunction. *Circulation.*, **110**, 3221–3228. https://doi.org/10.1161/01.CIR.0000147233.10318.23.

[36]. Ducharme, A., Libby, P., Lee, R.T., Ducharme, A., Frantz, S., Aikawa, M., Rabkin, E., Lindsey, M., Rohde, L.E., Schoen, F.J., Kelly, R.A., Werb, Z., Libby, P., Lee, R.T., (2000). Targeted deletion of matrix metalloproteinase-9 attenuates left ventricular enlargement and collagen accumulation after experimental myocardial infarction find the latest version : targeted deletion of matrix metalloproteinase-9 attenuates left ventricula. *J. Clin. Invest.*, **106**, 55–62.

[37]. Ramirez, T.A., Iyer, R.P., Ghasemi, O., Lopez, E.F., Levin, D.B., Zhang, J., Zamilpa, R., Chou, Y.M., Jin, Y.F., Lindsey, M.L., (2014). Aliskiren and valsartan mediate left ventricular remodeling post-myocardial infarction in mice through MMP-9 effects. *J. Mol. Cell. Cardiol.*, **72**, 326–335. https://doi.org/10.1016/j.yjmcc.2014.04.007.

[38]. Iyer, R.P., de Castro Brás, L.E., Patterson, N.L., Bhowmick, M., Flynn, E.R., Asher, M., Cannon, P.L., Deleon-Pennell, K.Y., Fields, G.B., Lindsey, M.L., (2016). Early matrix metalloproteinase-9 inhibition post-myocardial infarction worsens cardiac dysfunction by delaying inflammation resolution. *J. Mol. Cell. Cardiol.*, **100**, 109–117. https://doi.org/10.1016/j.yjmcc.2016.10.005.

[39]. van Putten, S., Shafieyan, Y., Hinz, B., (2015). Mechanical control of cardiac myofibroblasts. *J. Mol. Cell. Cardiol.*,. https://doi.org/10.1016/j.yjmcc.2015.11.025.

[40]. Kubota, A., Suto, A., Suzuki, K., Kobayashi, Y., Nakajima, H., (2019). Matrix metalloproteinase-12 produced by Ly6Clow macrophages prolongs the survival after myocardial infarction by preventing neutrophil influx. *J.*

*Mol. Cell. Cardiol.*, **131**, 41–52. https://doi.org/10.1016/j.yjmcc.2019.04.007.

[41]. Daseke, M.J., Tenkorang, M.A.A., Chalise, U., Konfrst, S. R., Lindsey, M.L., (2020). Cardiac fibroblast activation during myocardial infarction wound healing: fibroblast polarization after MI. *Matrix Biol.*, **91–92**, 109–116. https://doi.org/10.1016/j.matbio.2020.03.010.

[42]. Zeigler, A.C., Nelson, A.R., Chandrabhatla, A.S., Brazhkina, O., Holmes, J.W., Saucerman, J.J., (2020). Computational model predicts paracrine and intracellular drivers of fibroblast phenotype after myocardial infarction. *Matrix Biol.*, **91–92**, 136–151. https://doi.org/10.1016/j.matbio.2020.03.007.

[43]. Fu, X., Khalil, H., Kanisicak, O., Boyer, J.G., Vagnozzi, R. J., Maliken, B.D., Sargent, M.A., Prasad, V., Valiente-Alandi, I., Blaxall, B.C., Molkentin, J.D., (2018). Specialized fibroblast differentiated states underlie scar formation in the infarcted mouse heart. *J. Clin. Invest.*, **128**, 2127–2143. https://doi.org/10.1172/JCI98215.

[44]. Voloshenyuk, T.G., Landesman, E.S., Khoutorova, E., Hart, A.D., Gardner, J.D., (2011). Induction of cardiac fibroblast lysyl oxidase by TGF-β1 requires PI3K/Akt, Smad3, and MAPK signaling. *Cytokine.*, **55**, 90–97. https://doi.org/10.1016/j.cyto.2011.03.024.

[45]. Molkentin, J.D., Bugg, D., Ghearing, N., Dorn, L.E., Kim, P., Sargent, M.A., Gunaje, J., Otsu, K., Davis, J., (2017). Fibroblast-specific genetic manipulation of p38 mitogen-activated protein kinase in vivo reveals its central regulatory role in fibrosis. *Circulation*, **136**, 549–561. https://doi.org/10.1161/CIRCULATIONAHA.116.026238.

[46]. Xia, H., Nho, R.S., Kahm, J., Kleidon, J., Henke, C.A., (2004). Focal adhesion kinase is upstream of phosphatidylinositol 3-kinase/Akt in regulating fibroblast survival in response to contraction of type I collagen matrices via a beta 1 integrin viability signaling pathway. *J. Biol. Chem.*, **279**, 33024–33034. https://doi.org/10.1074/jbc.M313265200.

[47]. Aguado, B.A., Schuetze, K.B., Grim, J.C., Walker, C.J., Cox, A.C., Ceccato, T.L., Tan, A., Sucharov, C.C., Leinwand, L.A., Taylor, M.R.G., McKinsey, T.A., Anseth, K.S., (2019). Transcatheter aortic valve replacements alter circulating serum factors to mediate myofibroblast deactivation. *Sci. Transl. Med.*, **11** https://doi.org/10.1126/scitranslmed.aav3233. eaav3233.

[48]. Schroer, A.K., Ryzhova, L.M., Merryman, W.D., (2014). Network modeling approach to predict myofibroblast differentiation. *Cell. Mol. Bioeng.*, **7**, 446–459. https://doi.org/10.1007/s12195-014-0344-9.

[49]. Sun, M., Spill, F., Zaman, M.H., (2016). A computational model of YAP/TAZ mechanosensing. *Biophys. J.*, **110**, 2540–2550. https://doi.org/10.1016/j.bpj.2016.04.040.

[50]. Zeigler, A.C., Richardson, W.J., Holmes, J.W., Saucerman, J.J., (2016). A computational model of cardiac fibroblast signaling predicts context-dependent drivers of myofibroblast differentiation. *J. Mol. Cell. Cardiol.*, **94**, 72–81. https://doi.org/10.1016/j.yjmcc.2016.03.008.

[51]. Zeigler, A.C., Richardson, W.J., Holmes, J.W., Saucerman, J.J., (2016). Computational modeling of cardiac fibroblasts and fibrosis. *J. Mol. Cell. Cardiol.*, **93**, 73–83. https://doi.org/10.1016/j.yjmcc.2015.11.020.

[52]. Leonard-Duke, J., Evans, S., Hannan, R.T., Barker, T.H., Bates, J.H.T., Bonham, C.A., Moore, B.B., Kirschner, D. E., Peirce, S.M., (2020). Multi-scale models of lung fibrosis. *Matrix Biol.*, **91–92**, 35–50. https://doi.org/10.1016/j.matbio.2020.04.003.

[53]. Fowlkes, V., Clark, J., Fix, C., Law, B.A., Morales, M.O., Qiao, X., Ako-Asare, K., Goldsmith, J.G., Carver, W., Murray, D.B., Goldsmith, E.C., (2013). Type II diabetes promotes a myofibroblast phenotype in cardiac fibroblasts. *Life Sci.*, **92**, 669–676. https://doi.org/10.1016/J.LFS.2013.01.003.

[54]. Clark, R.A., Nielsen, L.D., Welch, M.P., McPherson, J.M., (1995). Collagen matrices attenuate the collagen-synthetic response of cultured fibroblasts to TGF-beta. *J. Cell Sci.*, **108**, 1251–1261.

[55]. Tuan, T.L., Song, A., Chang, S., Younai, S., Nimni, M.E., (1996). In vitro fibroplasia: matrix contraction, cell growth, and collagen production of fibroblasts cultured in fibrin gels. *Exp. Cell Res.*, **223**, 127–134. https://doi.org/10.1006/excr.1996.0065.

[56]. Grassl, E.D., Oegema, T.R., Tranquillo, R.T., (2002). Fibrin as an alternative biopolymer to type-I collagen for the fabrication of a media equivalent. *J. Biomed. Mater. Res.*, **60**, 607–612 http://www.ncbi.nlm.nih.gov/pubmed/11948519.

[57]. Cummings, C.L., Gawlitta, D., Nerem, R.M., Stegemann, J.P., (2004). Properties of engineered vascular constructs made from collagen, fibrin, and collagen–fibrin mixtures. *Biomaterials.*, **25**, 3699–3706. https://doi.org/10.1016/J.BIOMATERIALS.2003.10.073.

[58]. Roura, S., Gálvez-Montón, C., Bayes-Genis, A., (2017). Fibrin, the preferred scaffold for cell transplantation after myocardial infarction? An old molecule with a new life. *J. Tissue Eng. Regen. Med.*, **11**, 2304–2313. https://doi.org/10.1002/term.2129.

[59]. Nakamuta, J.S., Danoviz, M.E., Marques, F.L.N., dos Santos, L., Becker, C., Gonçalves, G.A., Vassallo, P.F., Schettert, I.T., Tucci, P.J.F., Krieger, J.E., (2009). Cell therapy attenuates cardiac dysfunction post myocardial infarction: effect of timing, routes of injection and a fibrin scaffold. *PLoS One*, **4**, https://doi.org/10.1371/journal.pone.0006005 e6005.

[60]. Foolen, J., Janssen-van den Broek, M.W.J.T., Baaijens, F.P.T., (2013). Synergy between Rho signaling and matrix density in cyclic stretch-induced stress fiber organization. *Acta Biomater.*,, 1–10. https://doi.org/10.1016/j.actbio.2013.12.001.

[61]. Foolen, J., Deshpande, V.S., Kanters, F.M.W., Baaijens, F.P.T., (2012). The influence of matrix integrity on stress-fiber remodeling in 3D. *Biomaterials.*, **33**, 7508–7518. https://doi.org/10.1016/j.biomaterials.2012.06.103.

[62]. Liu, M., Sun, J., Sun, Y., Bock, C., Chen, Q., (2009). Thickness-dependent mechanical properties of polydimethylsiloxane membranes. *J. Micromech. Microeng.*, **19**, 4. https://doi.org/10.1088/0960-1317/19/3/035028.

[63]. Berton, A., Emonard, H., Hornebeck, W., Bellon, G., Lorimier, S., Laurent-Maquin, D., (2000). Contribution of the plasmin/matrix metalloproteinase cascade to the retraction of human fibroblast populated collagen lattices. *Mol. Cell Biol. Res. Commun.*, **3**, 173–180. https://doi.org/10.1006/mcbr.2000.0210.

[64]. Bertram, H., Boeuf, S., Wachters, J., Boehmer, S., Heisel, C., Hofmann, M.W., Piecha, D., Richter, W., (2009). Matrix metalloprotease inhibitors suppress initiation and progression of chondrogenic differentiation of mesenchymal stromal cells in vitro. *Stem Cells Dev.*, **18**, 881–892. https://doi.org/10.1089/scd.2008.0306.

[65]. Leask, A., (2010). Potential therapeutic targets for cardiac fibrosis: TGFβ, angiotensin, endothelin, CCN2, and PDGF, partners in fibroblast activation. *Circ. Res.*, **106**,

1675–1680. https://doi.org/10.1161/CIRCRESAHA.110.217737.
[66]. von Lueder, T.G., Wang, B.H., Kompa, A.R., Huang, L., Webb, R., Jordaan, P., Atar, D., Krum, H., (2015). Angiotensin receptor Neprilysin inhibitor LCZ696 attenuates cardiac remodeling and dysfunction after myocardial infarction by reducing cardiac fibrosis and hypertrophy. *Circ. Heart Fail.*, **8**, 71–78. https://doi.org/10.1161/CIRCHEARTFAILURE.114.001785.
[67]. Burke, R.M., Lighthouse, J.K., Mickelsen, D.M., Small, E. M., (2019). Sacubitril/valsartan decreases cardiac fibrosis in left ventricle pressure overload by restoring PKG signaling in cardiac fibroblasts. *Circ. Heart Fail.*, **12**, 1–15. https://doi.org/10.1161/CIRCHEARTFAILURE.118.005565.
[68]. Gallini, R., Lindblom, P., Bondjers, C., Betsholtz, C., Andrae, J., (2016). PDGF-A and PDGF-B induces cardiac fibrosis in transgenic mice. *Exp. Cell Res.*, **349**, 282–290. https://doi.org/10.1016/j.yexcr.2016.10.022.
[69]. Zymek, P., Bujak, M., Chatila, K., Cieslak, A., Thakker, G., Entman, M.L., Frangogiannis, N.G., (2006). The role of platelet-derived growth factor signaling in healing myocardial infarcts. *J. Am. Coll. Cardiol.*, **48**, 2315–2323. https://doi.org/10.1016/j.jacc.2006.07.060.
[70]. Bujak, M., Frangogiannis, N., (2007). The role of TGF-β signaling in myocardial infarction and cardiac remodeling. *Cardiovasc. Res.*, **74**, 184–195. https://doi.org/10.1016/j.cardiores.2006.10.002.
[71]. Ikeuchi, M., Tsutsui, H., Shiomi, T., Matsusaka, H., Matsushima, S., Wen, J., Kubota, T., Takeshita, A., (2004). Inhibition of TGF-B signaling exacerbates early cardiac dysfunction but prevents late remodeling after infarction. *Cardiovasc. Res.*, **64**, 526–535. https://doi.org/10.1016/j.cardiores.2004.07.017.
[72]. Abbate, A., Van Tassell, B.W., Biondi-Zoccai, G., Kontos, M.C., Grizzard, J.D., Spillman, D.W., Oddi, C., Roberts, C.S., Melchior, R.D., Mueller, G.H., Abouzaki, N.A., Rengel, L.R., Varma, A., Gambill, M.L., Falcao, R.A., Voelkel, N.F., Dinarello, C.A., Vetrovec, G.W., (2013). Effects of interleukin-1 blockade with anakinra on adverse cardiac remodeling and heart failure after acute myocardial infarction [from the virginia commonwealth university-anakinra remodeling trial (2) (vcu-art2) pilot study]. *Am. J. Cardiol.*, **111**, 1394–1400. https://doi.org/10.1016/j.amjcard.2013.01.287.
[73]. Li, Y.Y., Feng, Y.Q., Kadokami, T., McTiernan, C.F., Draviam, R., Watkins, S.C., Feldman, A.M., (2000). Myocardial extracellular matrix remodeling in transgenic mice overexpressing tumor necrosis factor α can be modulated by anti-tumor necrosis factor α therapy. *Proc. Natl. Acad. Sci. U. S. A.*, **97**, 12746–12751. https://doi.org/10.1073/pnas.97.23.12746.
[74]. Liu, W., Wang, X., Gong, J., Mei, Z., Gao, X., Zhao, Y., Ma, J., Qian, L., (2014). The stress-related hormone norepinephrine induced upregulation of nix, contributing to ECM protein expression. *Cell Stress Chaperones*, **19**, 903–912. https://doi.org/10.1007/s12192-014-0515-6.
[75]. Peng, J.F., Gurantz, D., Tran, V., Cowling, R.T., Greenberg, B.H., (2002). Tumor necrosis factor-α-induced AT1 receptor upregulation enhances angiotensin II-mediated cardiac fibroblast responses that favor fibrosis. *Circ. Res.*, **91**, 1119–1126. https://doi.org/10.1161/01.RES.0000047090.08299.D5.
[76]. Gao, X., He, X., Luo, B., Peng, L., Lin, J., Zuo, Z., (2009). Angiotensin II increases collagen I expression via transforming growth factor-beta1 and extracellular signal-regulated kinase in cardiac fibroblasts. *Eur. J. Pharmacol.*, **606**, 115–120. https://doi.org/10.1016/j.ejphar.2008.12.049.
[77]. Lai, K.-B., Sanderson, J.E., Yu, C.-M., (2013). The regulatory effect of norepinephrine on connective tissue growth factor (CTGF) and vascular endothelial growth factor (VEGF) expression in cultured cardiac fibroblasts. *Int. J. Cardiol.*, **163**, 183–189. https://doi.org/10.1016/j.ijcard.2011.06.003.
[78]. Schneider, C.A., Rasband, W.S., Eliceiri, K.W., (2012). NIH image to ImageJ: 25 years of image analysis. *Nat. Methods*, **9**, 671–675. https://doi.org/10.1038/nmeth.2089.
[79]. Zhao, Y., Rafatian, N., Feric, N.T., Cox, B.J., Aschar-Sobbi, R., Wang, E.Y., Aggarwal, P., Zhang, B., Conant, G., Ronaldson-Bouchard, K., Pahnke, A., Protze, S., Lee, J.H., Davenport Huyer, L., Jekic, D., Wickeler, A., Naguib, H.E., Keller, G.M., Vunjak-Novakovic, G., Broeckel, U., Backx, P.H., Radisic, M., (2019). A platform for generation of chamber-specific cardiac tissues and disease modeling. *Cell*, **176** https://doi.org/10.1016/j.cell.2018.11.042. 913–927.e18.
[80]. McQuin, C., Goodman, A., Chernyshev, V., Kamentsky, L., Cimini, B.A., Karhohs, K.W., Doan, M., Ding, L., Rafelski, S.M., Thirstrup, D., Wiegraebe, W., Singh, S., Becker, T., Caicedo, J.C., Carpenter, A.E., (2018). CellProfiler 3.0: next-generation image processing for biology. *PLoS Biol.*, **16** https://doi.org/10.1371/journal.pbio.2005970. e2005970.
[81]. de Boer, R.A., De Keulenaer, G., Bauersachs, J., Brutsaert, D., Cleland, J.G., Diez, J., Du, X.-J., Ford, P., Heinzel, F.R., Lipson, K.E., McDonagh, T., Lopez-Andres, N., Lunde, I.G., Lyon, A.R., Pollesello, P., Prasad, S.K., Tocchetti, C.G., Mayr, M., Sluijter, J.P.G., Thum, T., Tschöpe, C., Zannad, F., Zimmermann, W.-H., Ruschitzka, F., Filippatos, G., Lindsey, M.L., Maack, C., Heymans, S., (2019). Towards better definition, quantification and treatment of fibrosis in heart failure. A scientific roadmap by the Committee of Translational Research of the Heart Failure Association (HFA) of the European Society of Cardiology. *Eur. J. Heart Fail.*, **21**, 272–285. https://doi.org/10.1002/ejhf.1406.
[82]. López, B., González, A., Lindner, D., Westermann, D., Ravassa, S., Beaumont, J., Gallego, I., Zudaire, A., Brugnolaro, C., Querejeta, R., Larman, M., Tschöpe, C., Díez, J., (2013). Osteopontin-mediated myocardial fibrosis in heart failure: a role for lysyl oxidase? *Cardiovasc. Res.*, **99**, 111–120. https://doi.org/10.1093/cvr/cvt100.
[83]. Kaur, H., Takefuji, M., Ngai, C.Y., Carvalho, J., Bayer, J., Wietelmann, A., Poetsch, A., Hoelper, S., Conway, S.J., Möllmann, H., Looso, M., Troidl, C., Offermanns, S., Wettschureck, N., (2016). Targeted ablation of Periostin-expressing activated fibroblasts prevents adverse cardiac remodeling in mice. *Circ. Res.*, **118**, 1906–1917. https://doi.org/10.1161/CIRCRESAHA.116.308643.
[84]. Kanisicak, O., Khalil, H., Ivey, M.J., Karch, J., Maliken, B. D., Correll, R.N., Brody, M.J., Lin, S.C.J., Aronow, B.J., Tallquist, M.D., Molkentin, J.D., (2016). Genetic lineage tracing defines myofibroblast origin and function in the injured heart. *Nat. Commun.*, **7**, 1–14. https://doi.org/10.1038/ncomms12260.
[85]. Bates, D., Mächler, M., Bolker, B., Walker, S., (2015). Fitting linear mixed-effects models using lme4. *J. Stat. Softw.*, **67**, 201–210. https://doi.org/10.18637/jss.v067.i01.